Hindawi
Advances in Materials Science and Engineering
Volume 2021, Article ID 7754523, 9 pages
https://doi.org/10.1155/2021/7754523

Research Article

Sonoelectrochemical Synthesis of Antibacterial Active Silver Nanoparticles in Rhamnolipid Solution

Mariana Shepida, Orest Kuntyi, Martyn Sozanskyi, and Yuriy Sukhatskiy

Lviv Polytechnic National University, Lviv 79013, Ukraine

Correspondence should be addressed to Mariana Shepida; maryana_shepida@ukr.net

Received 27 April 2021; Revised 26 May 2021; Accepted 27 May 2021; Published 15 June 2021

Academic Editor: Ştefan Ţălu

The results of studies of the synthesis of AgNPs colloidal solutions by cyclic voltammetry (E from +1.0 to −1.0 V) in rhamnolipid (RL) solutions and the use of soluble anodes in the ultrasound field (22 kHz) are presented. It is shown that the algorithm of anodic dissolution—reduction of Ag(I)—nucleation, and formation of AgNPs makes it possible to obtain nanoparticles with the size from 1 nm to 3 nm. It was found that with an increase in the RL concentration from 1 g/L to 4 g/L, the anodic and cathodic currents increase as well as the rate of AgNPs formation, respectively. The rate of nanoparticles formation also increases with an increase in temperature from 20°C to 60°C, and it corresponds to the diffusion-kinetic range of action of this factor. Moreover, the size of AgNPs depends little on the temperature. The character of the UV-Vis pattern of AgNPs colloidal solutions in RL (with an absorption maximum of 415 nm) is the same over a wide range of nanoparticle concentrations. The curves practically do not change in time, which indicate the stability of anodic and cathodic processes during prolonged sonoelectrochemical synthesis. The cyclic voltammetry curves practically do not change in time, which indicate the stability of anodic and cathodic processes during prolonged sonoelectrochemical synthesis. The antimicrobial activity of synthesized AgNPs solutions to strains of *Escherichia coli*, *Candida albicans*, and *Staphylococcus aureus* was established.

1. Introduction

Silver nanoparticles (AgNPs) are widely used in pharmacy, cosmetics, anti-infective therapy, and the textile industry [1, 2]; they are promising in sensorics [3], in antibacterial galvanic metal [4] and alloy [5] composite coatings, and catalysis [6]. Physicochemical properties of nanoparticles significantly depend on their geometry [6–10]. So, controlled synthesis in shape and size is one of the priority areas of nanochemistry of metal nanoparticles (MNPs) in the last decade [11–14]. The nucleation and growth of nanoparticles in solution are multistage processes [15–18], and their course depends on many factors. Among the latter, the concentration of precursors (metal ions, surfactant, and its ratios) [11, 12, 14, 16], pH of solution [13, 16], temperature [16], and especially, the transport effect [18] are important. The action of these factors is due to the synthesis methods, among which the most promising in the aspect of processes controllability is electrochemical [19–24]. They also meet to the criteria of "green" technologies. A hybrid one, which combines electrochemical and sonochemical processes, is sonoelectrochemical synthesis [25–30].

Sonoelectrochemical synthesis of metal nanoparticles includes electrochemical reduction of metal ions with their subsequent removal from the cathode surface. A combination of sequential pulse electrolysis and pulse sonolysis is often used for this [25, 27]. Moreover, during a current impulse (τon), MNPs are formed on the cathode surface, which are "shaken off" from it during the ultrasound period (τUS). So, the controlled synthesis of nanoparticles by geometry is carried out according to the algorithm of time of electrolysis (τon) ⟶ time of ultrasound (τUS) pause of electrolysis and ultrasound (τoff). Moreover, the main parameters of the influence are τon and the value of the cathode current (icathode), τUS, and the concentration of metal ions [25, 27, 31]. The sonoelectrochemical synthesis in

surfactant solutions by cyclic voltammetry and the use of sacrificial anodes is promising [30]. It allows providing an algorithm for the concentration of metal ions due to the anodic reaction.

$$M_{(solid)} \longrightarrow M^{n}{}_{+(solution)} + ne \quad (1)$$

When using an ultrasonic field due to the collapse of cavitation bubbles, which accompanied by the appearance of local zones with extreme temperatures and pressures, the water sonolysis occurs (2) and decomposition of surfactant molecules (3) with the formation of radicals [29]. The latter, primarily $H^{\bullet}$ (4) and $R^{\bullet}$ (5), are involved in the reduction of M^{n+} ions to M^{0} atoms with the subsequent formation of MNPs. So, at sonoelectrochemical synthesis of MNPs, ultrasound performs a dual function: (1) "shaking" nanoparticles from the cathode surface and (2) sonolysis of water and surfactant with the formation of radicals, which lead to the reduction of metal ions and the formation of nanoparticles in solution.

$$H_2O \longrightarrow))) H^{\bullet}, {}^{\bullet}OH, HO_2^{\bullet} \quad (2)$$

$$R - H \longrightarrow)))R^{\bullet} + H^{\bullet} \quad (3)$$

$$nH^{\bullet} + M^{n+} \longrightarrow nH^{+} + M^{0} \quad (4)$$

$$nR^{\bullet} + M^{n+} \longrightarrow MnR' + M^{0} + nH^{+} \quad (5)$$

Sonoelectrochemical synthesis of AgNPs is carried out in solutions containing surfactants that act as nanoparticles stabilizers (Table 1). However, these are mainly polymeric organic substances containing an electrodonating atom. With its participation, a surface complex of surfactants-AgNPs is formed.

The aim of the work is to establish the effect of ultrasound on the formation of AgNPs by cyclic voltammetry in rhamnolipid solutions with the use of sacrificial anode. Rhamnolipids are microbial biosurfactants, a natural surface-active agent that exhibits antibacterial activity and biodegradable properties [37–39]. It is known that rhamnolipids form complexes with metal ions [40–43] and are effective stabilizers of AgNPs [24, 44–47]. Therefore, the work is aimed at controlled "green" synthesis of small silver nanoparticles.

2. Experimental

Sonoelectrochemical synthesis of colloidal solutions of silver nanoparticles was performed using a standard trielectrode electrochemical cell with a volume of 50 ml and MTech PGP-550M potentiostat. Two identical silver plates ($S = 14.4\ cm^2$) performed the functions of working and auxiliary electrodes at the same time in cyclic voltammetry. The reference electrode was a silver chloride Ag/AgCl electrode with a Luggin capillary containing 1 mol/L of KNO3. Studies of the electrochemical behavior of silver and the synthesis of AgNPs were carried out using cyclic voltammetry in RL solutions with a concentration from 1 to 4 g/L at pH = 9.0, and temperature was changed from 20°C to 60°C. The sweep rate of the cyclic voltammetry potential is 50 mV/s in the E range from +1.0 to −1.0 V. For sonoelectrochemical synthesis of colloidal solutions of silver nanoparticles, an ultrasonic emitter of magnetostrictive-type was used. The frequency of ultrasonic radiation was 22 kHz. Useful specific power of ultrasonic radiation was from 40 to 62.5 W/L. Isothermal conditions for sonoelectrochemical synthesis of colloidal solutions of silver nanoparticles were provided by the UTU-4 ultrathermostat. The samples of solutions were analyzed using the UV-3100PC UV-Vis-spectrophotometer (Shanghai Mapada Instruments Co., Ltd. (China)) in quarts cuvettes 1 cm in thickness in the wavelength region from 190 to 1100 nm with maximum absorption at $\lambda = 415$ nm.

TEM images of the samples were recorded using a JEM-I230 (JEOL, Tokyo, Japan) with an acceleration voltage of 80 kV. The samples for TEM investigations were prepared by drying 0.05 μL of silver sol on the carbon grid at room temperature. The diameters of obtained AgNPs were determined using TEM images by comparing individual particles' sizes with the scales presented on images. The statistical histograms were obtained using Origin software pack with its standard deviation values of nanoparticle size. Additionally, NPs size and density were determined by using the public domain Java image processing program ImageJ2 [48]. Theoretical calculations and processing of experimental data are created by means of the software (Inconico Screen Calipers 4.0, OriginPro 8.0).

The antibacterial activity of AgNPs was evaluated against Gram-negative *Escherichia Coli* (*E. coli*) and Gram-positive bacteria *Staphylococcus aureus* (*S. aureus*) and *Candida albicans* (*C. albicans*). To do this, the bacteria were inoculated into Petri dishes with a solid selective nutrient medium for each species of microorganisms: yellow-salt agar, for the culture of *S. aureus*, Endo agar, for the culture of *E. coli*, and agar Saburo, for *Candida albicans* . Inoculation was performed after 1, 6, 18, and 48 hours of contact of bacteria with AgNPs solution. All the biological material was incubated at 37°C for 24 hours in a bacteriological incubator. Antibacterial activity was indexed by percentages of inhibition, colony-forming units per mL (CFU/mL). Hence, the initial concentration is *E. coli*, 110 CFU/mL, *S. aureus*, 230 CFU/mL, *Candida albicans*, 70 CFU/mL.

3. Results and Discussion

Sonoelectrochemical synthesis of AgNPs by cyclic voltammetry in rhamnolipid solutions with the use of silver anode goes through the algorithm of anodic dissolution—reduction of Ag(I)—nucleation, and formation of AgNPs. All three stages proceed with the participation of the surfactant in the ultrasonic field. Due to the oxygen electrodonor atom, adsorption of RL molecules on the anodic surface occurs, and the $[AgRL]^{+}$ rhamnolipid complex is formed upon dissolution of silver (6). The $[AgRL]^{+}$ complex participates in cathodic reduction (7) and reduction by radicals (7a), as well as in the formation and stabilization of nanoclusters (AgNCs) and AgNPs.

Table 1: Conditions for the sonoelectrochemical synthesis of silver nanoparticles.

Precursors	Stabilizer (surfactant)	Ultrasound parameters	λ_{max} (nm)	AgNPs size (nm)	References
Sacrificial anode	NaPa	22 kHz, 40, . . ., 62.5 W·dm^{-3}	500	4–30	[30]
$AgNO_3$	NTA	60 W·cm^{-2}	413	Nanorods, $\varnothing = 10$–20	[31]
$AgNO_3$	EDTA	50 kHz, 100 W	—	$\varnothing = 80$, >15 μm long	[32]
$AgNO_3$	NTA	Pulse US, 750 W	—	5 ± 2, 60 ± 30, 75 ± 25	[33]
$Ag_3C_6H_5O_7$	PVP	Pulse US, 22 kHz	410	20–25	[34]
$AgClO_4$	PVP	40 kHz, 50 W	415–426	7–10	[35]
$AgNO_3$	SDS	Pulse US, 100 W·cm^{-2}	401, 418	~20	[36]

NaPa, sodium polyacrylate; NTA, nitrilotriacetate; EDTA, ethylenediamine tetraacetic acid; PVP, polyvinylpyrrolidone; SDS, sodium dodecyl sulfate.

$$\text{Anodic dissolution}: \ \mathrm{Ag}_{(\text{solid})} + \mathrm{RL} \longrightarrow))) \left[\mathrm{AgRL}\right]^{+}_{(\text{solution})} + \mathrm{e} \tag{6}$$

$$\text{Reduction of Ag(I)}: \left[\mathrm{AgRL}\right]^{+}_{(\text{solution})} + \mathrm{e} \longrightarrow))) \left[\mathrm{Ag(0)RL}\right]_{(\text{solution})} \tag{7}$$

$$\left[\mathrm{AgRL}\right]^{+}_{(\text{solution})} + H^{\bullet}\left(R^{\bullet}\right) \longrightarrow))) \left[\mathrm{Ag(0)RL}\right]_{(\text{solution})} + \mathrm{H} + \left(\mathrm{R}'\right) \tag{7a}$$

$$\mathrm{m}\left[\mathrm{Ag(0)RL}\right]_{(\text{solution})} \longrightarrow))) \left[\mathrm{AgNCsRL}\right] \longrightarrow \cdots \longrightarrow \left[\mathrm{AgNPsRL}\right] \tag{8}$$

A consequence of the ultrasound action in these stages is the formation of small in size AgNPs with a relatively small scatter in the value of this quantity (Figure 1), which indicates a predominant nucleation rate as compared to the growth of nanoparticles. This is due to the intensification of diffuse processes under the influence of acoustic cavitation and the implementation of "soft" mixing of the entire volume of the reaction medium. So, ultrasound accelerates the reduction of $[AgRL]^+$ ions following reactions (7) and (7a) and the formation of AgNCs and AgNPs stabilized by rhamnolipid. So, ultrasound accelerates the reduction processes of $[AgRL]^+$ ions by (7) and (7a) reactions and the formation of rhamnolipid-stabilized AgNCs and AgNPs.

The stability of the first two stages of the algorithm of sonoelectrochemical synthesis of AgNPs, namely, the process of anodic dissolution of silver (6) and cathodic reduction of $[AgRL]^+$ ions (7), is confirmed by the practical reproducibility of cyclic volt-ampere curves during long-term electrolysis (Figure 2).

The stability of the sonoelectrochemical synthesis of AgNPs, including (6)–(8) processes, is confirmed by the almost linear dependence of the optical density (O.D.) over time (Figure 3). Moreover, the wavelength value (415 nm) of O.D. maximums (λ_{max}) does not change during sonoelectrolysis and long-term storage of solutions (two months). The range (from 300 to 600 nm) also does not change. All these indicate the stability of geometry of the synthesized nanoparticles.

With an increase in the concentration of rhamnolipid, the anodic current densities increase, which is identical to the rate of silver dissolution (Figure 4(a)). Such regularity is observed even without an ultrasonic field [24]. It is also characteristic in solutions of polymeric surfactants, for example, NaPA [23]. This is due to the complexation of Ag^+ ions during (6) reaction, where increasing the ligand (RL) concentration promotes to accelerate the process. Accordingly, the rate of sonoelectrochemical synthesis of AgNPs increases (Figure 4(b)), which includes cathodic (7) and sonochemical (7a) reduction of Ag(I) from $[AgRL]^+$ complexes. Moreover, the λmax value is practically independent of the RL concentration in the solution.

With increasing the temperature, there is a tendency to increase in the values of anodic current densities; however, a clear temperature dependence of this value was not found (Figure 5(a)). This is due to the simultaneous action of many factors, among which, first of all, such as the following: increasing electrical conductivity, improving diffusion, and weakening the adsorption of rhamnolipid molecules on the anodic surface. The consequence of the increasing in anodic currents is an increase in the values of cathodic currents and the rate of sonoelectrochemical synthesis of AgNPs (Figure 5(b)).

The character of the absorption spectra and the λmax values (Figure 5(b)) practically do not change with increasing temperature, that is, indirect evidence of the insignificant relationship between AgNPs geometry and this factor. Confirmation is the temperature dependence of the size of nanoparticles by sonoelectrochemical synthesis, where a significant increase is not observed in the range from 20 to 60°C (Figure 6). For comparison, in electrochemical synthesis, the influence of temperature factor is significant [24]. Thus, ultrasound provides a high rate of (7) and (7a) reactions and leads to almost complete reduction of $[AgRL]^+$ ions in the cathodic period of cyclic voltammetry. This promotes the predominant nucleation process (8) and prevents appreciable growth of AgNPs.

4. Antibacterial Activity of Synthesized AgNPs (Antibacterial Study)

The results of studies of the antibacterial properties of sonoelectrochemically synthesized AgNPs indicate their activity against Gram-positive bacteria of *Staphylococcus aureus* ATCC 25923 and Gram-negative bacteria of *Escherichia coli* ATCC 25922 (Table 2) and fungicidal bacteria of *Candida albicans* ATCC 885-653 (Table 3).

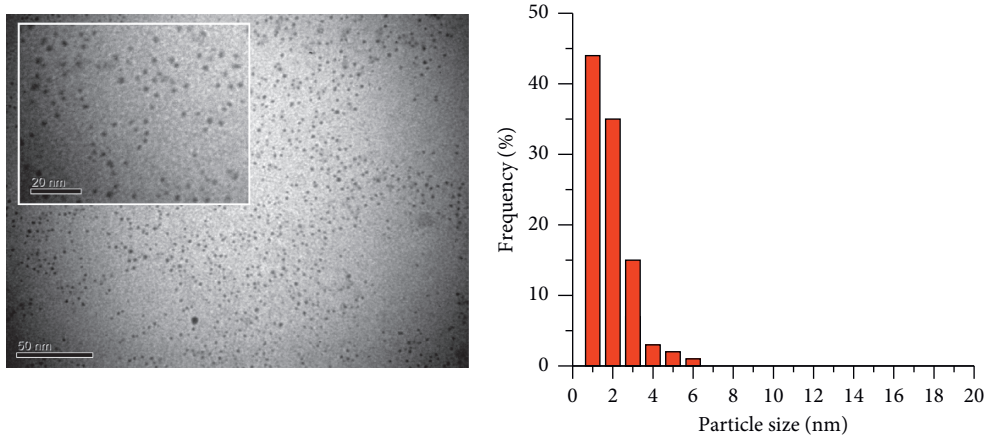

Figure 1: TEM images (a) and the size distribution histograms (b) of AgNPs, synthesized in RL solution (2 g/L) at 40 cycles, $t = 20^{\circ}$C.

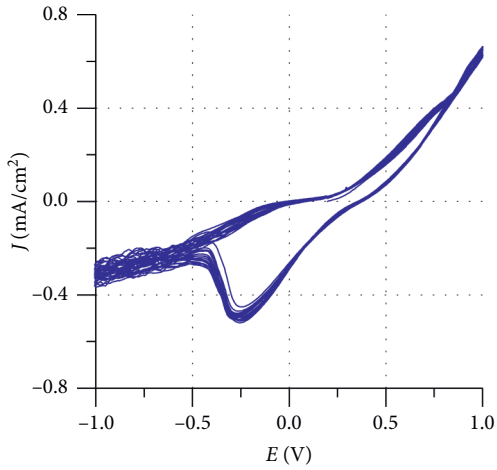

Figure 2: Array of cyclic voltamperograms of silver in RL solution (2 g/L), $t = 20^{\circ}$C, 20 cycles.

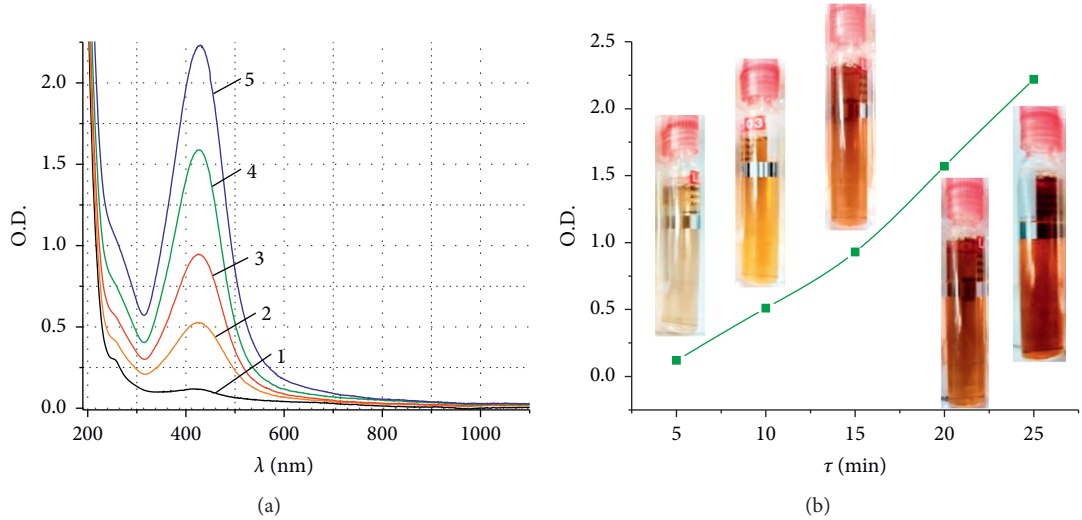

Figure 3: Spectral dependences of optical absorption of AgNPs obtained by sonoelectrochemical synthesis (a) at different process durations (min): 1–5; 2–10; 3–15; 4–20; and 5–25 and (b) change of O.D. maximum and color over time.

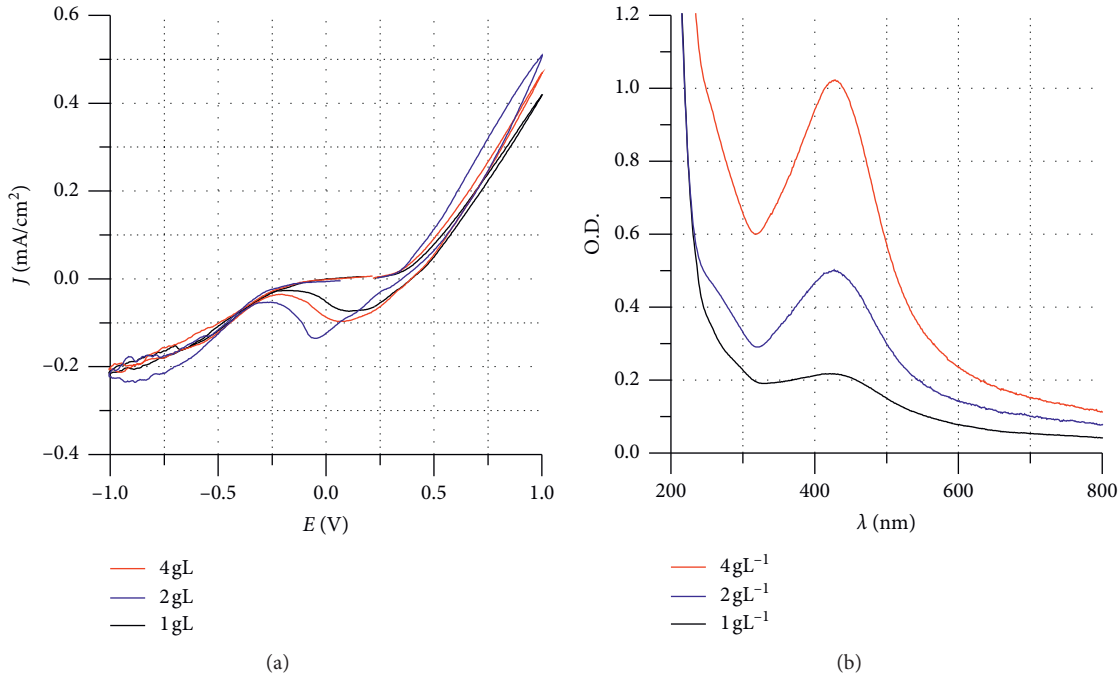

Figure 4: Cyclic voltamperograms (a) and spectral dependences of optical absorption (b) of AgNPs, synthesized ultrasonically in an aqueous solution of RL (1, . . ., 4 g/L) at the temperature of $t = 20^{\circ}$C and the process duration of 20 cycles.

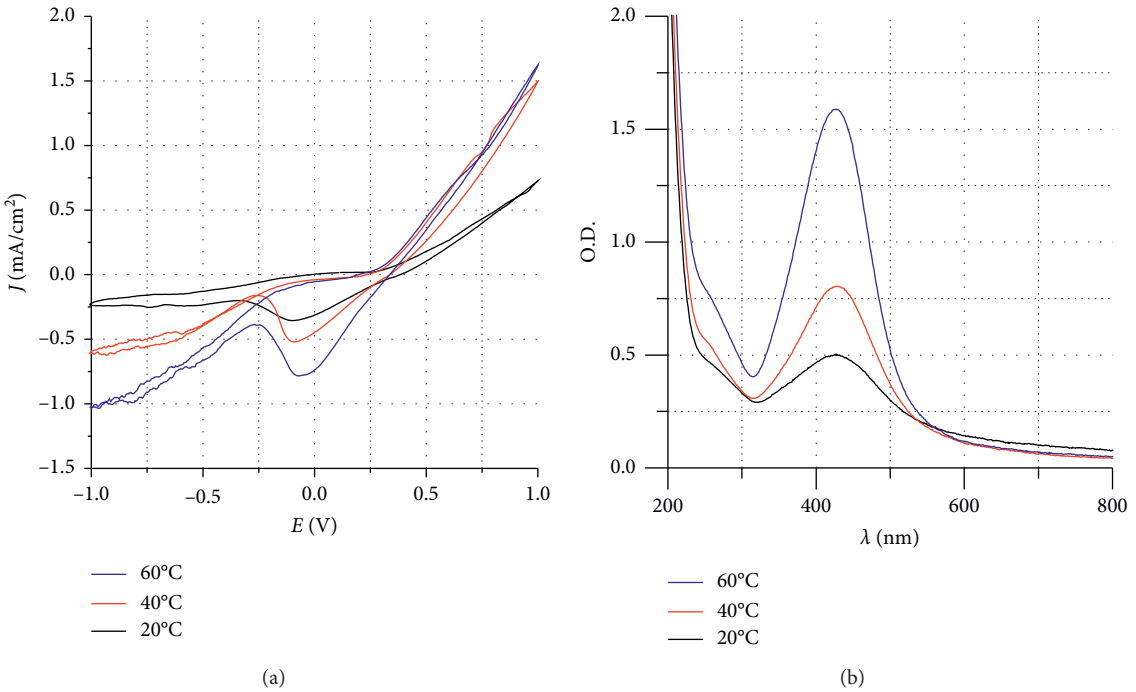

Figure 5: Cyclic voltamperograms (a) and spectral dependences of optical absorption (b) of AgNPs, synthesized ultrasonically in an aqueous solution of RL (2 g/L) at the temperature of $t = 20$, 40, and 60°C and the process duration of 20 cycles.

The antimicrobial properties of AgNPs can be explained by two different mechanisms: (1) fixation of AgNPs on cell membranes, followed by their penetration into the cell and damage to the membrane with the release of the cell contents (the so-called "Trojan horse mechanism") [49], and (2) release of Ag^{+} ions, which have antimicrobial properties.

The antibacterial (disinfection) effect of AgNPs colloidal solutions synthesized by the sonoelectrochemical method at 20°C is absolute for strains of *Escherichia coli* ATCC 25922 and *Candida albicans* ATCC 885-653 (Figure 7).

Antibacterial and fungicidal properties of the synthesized AgNPs solutions can be caused by two different

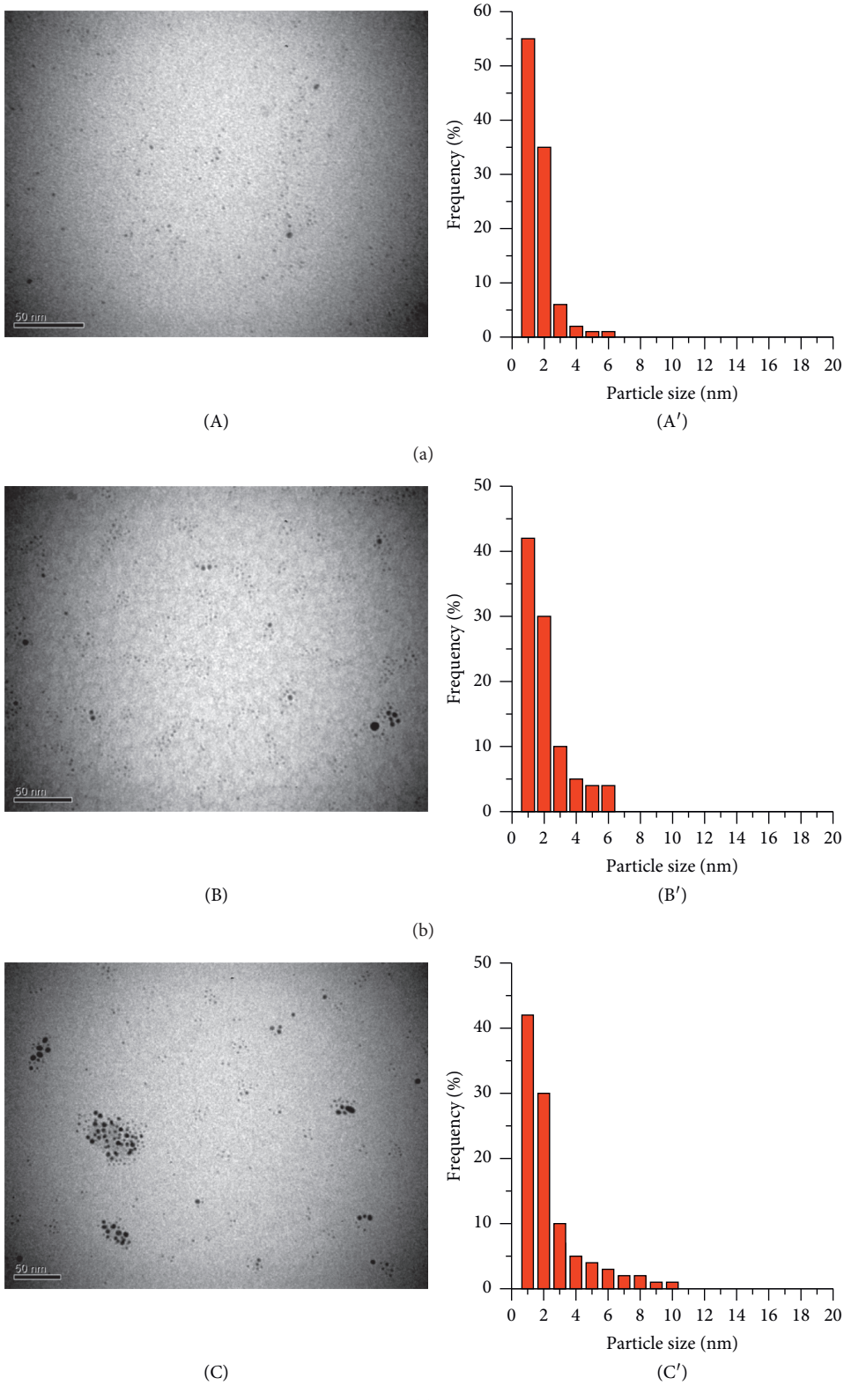

Figure 6: TEM images (A, B, C) and the size distribution histograms (A′, B′, C′) of AgNPs, synthesized in RL solution (2 g/L) at $t = 20$ (a), 40 (b), and 60°C (c).

Table 2: Antibacterial properties of colloidal solutions of silver nanoparticles synthesized by the sonoelectrochemical method and stabilized with rhamnolipid solution.

Species of bacteria	Exposure time (h)	Quantity CFU (cm^3)	Bactericidal action	Percentages of inhibition (%)
S. aureus ATCC 25923 (F-49)	1	230	–	0
	6	60	–	73.9
	18	Not found	+	100
	48	Not found	+	100
E. coli ATCC 25922 (F-50)	1	110	–	0
	6	Not found	+	100
	18	Not found	+	100
	48	Not found	+	100

CFU, colony-forming units; +, pronounced antimicrobial (disinfecting) effect (no growth of microorganisms); –, no antimicrobial (disinfectant) action (available growth of microorganisms).

Table 3: Fungicidal properties of colloidal solutions of silver nanoparticles synthesized by the sonoelectrochemical method and stabilized with rhamnolipid solution.

Species of mushrooms	Exposure time (h)	Quantity CFU (cm^3)	Bactericidal action	Percentages of inhibition (%)
Candida albicans ATCC 885–653	1	70	–	0
	6	30	–	57.1
	18	5	–	92.9
	48	Not found	+	100

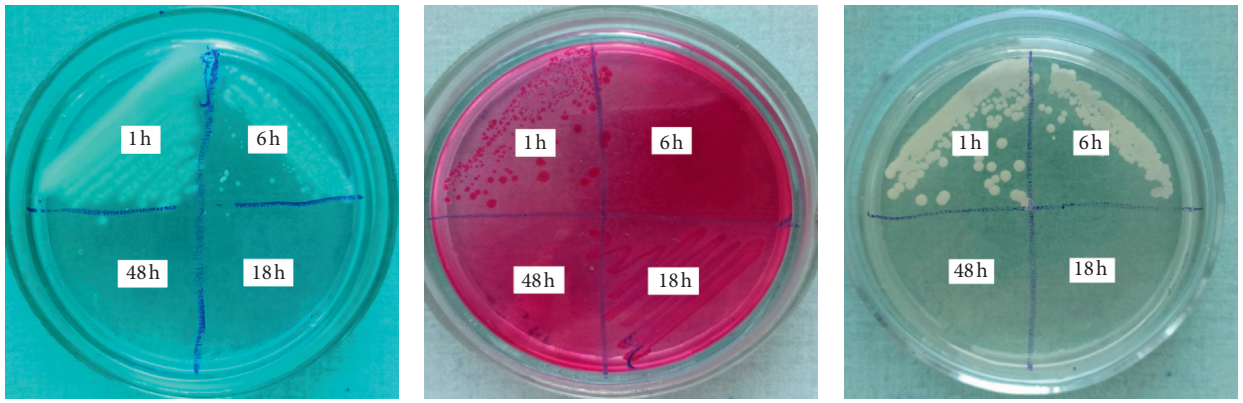

(a) (b) (c)

Figure 7: Photos of Petri dishes, illustrating the bactericidal effect of AgNPs solutions, stabilized with rhamnolipid solution, in relation to (a) *Staphylococcus* aureus ATCC 25923, (b) *Escherichia coli* ATCC 25922, and (c) *Candida albicans* ATCC 885-653.

mechanisms: 1, fixation of silver nanoparticles on cell membranes, the interaction of AgNPs from the protein component of the membrane, which leads to its damage, and accordingly, the introduction of cell contents; 2, release of Ag + ions, which have bactericidal and fungicidal properties. The high affinity of AgNPs with phosphorus and sulphur is the main reason of their antibacterial effect. Cell membrane has a lot of sulphur-containing proteins. The cell viability of bacteria could be destroyed by AgNPs, when they react with sulphur-containing amino acids outside or inside the cell membrane. They also investigated that silver ions from the AgNPs react with phosphorous, which results in the stopping of DNA replication or reaction with sulphur-containing proteins, that inhibits the enzyme functions [50]. In general, the diameter of AgNPs is <10 nm, and they attack the sulphur-containing proteins of bacteria and leads to penetrability of the cell membrane and later death of bacteria [51]. AgNPs with a diameter <10 nm makes pores on the cell walls of bacteria. This leads to cell death by realising cytoplasmic content without changing of extracellular and intracellular nucleic acids and proteins of bacterium [52].

5. Conclusions

Cyclic voltammetry E from +1.0 to −1.0 V in solutions of rhamnolipid, natural origin surfactant, and using the ultrasonic field (22 kHz) and the sacrificial anode allow to realize "green" synthesis of stabilized silver nanoparticles to the algorithm of anodic dissolution—reduction of Ag(I)—nucleation and formation of AgNPs. This provides controlled production of nanoparticles from 1 to 3 nm in size in a wide range of RL concentrations (from 1 to 4 g/L) and temperatures (from 20 to 60°C). The rate of AgNPs synthesis

increases with increasing surfactant concentration and temperature, which is due to the acceleration of anodic dissolution of silver. Sonoelectrochemically obtained AgNPs colloidal solutions show antimicrobial activity to Staphylococcus aureus, Escherichia coli, and Candida albicans.

Data Availability

The data used to support the findings of this study are included within the article.

Conflicts of Interest

The authors declare that there are no conflicts of interest.

Acknowledgments

This work was carried out with the partial financial support of the National Research Foundation of Ukraine (project registration number: 2020.02/0309) ("Design of polyfunctional nanostructured mono- and bimetals with electrocatalytic and antimicrobial properties").

References

[1] C. Liao, Y. Li, and S. Tjong, "Bactericidal and cytotoxic properties of silver nanoparticles," *International Journal of Molecular Sciences*, vol. 20, no. 2, pp. 449–495, 2019.

[2] O. Gherasim, R. A. Puiu, A. C. Bîrcă, A.-C. Burduşel, and A. M. Grumezescu, "An updated review on silver nanoparticles in biomedicine," *Nanomaterials*, vol. 10, no. 11, pp. 2318–2361, 2020.

[3] B. Calderón-Jiménez, M. E. Johnson, A. R. Montoro Bustos, K. E. Murphy, M. R. Winchester, and J. R. Vega Baudrit, "Silver nanoparticles: technological advances, societal impacts, and metrological challenges," *Frontiers in Chemistry*, vol. 5, 2017.

[4] A. Méndez-Albores, S. G. González-Arellano, Y. Reyes-Vidal et al., "Electrodeposited chrome/silver nanoparticle (Cr/AgNPs) composite coatings characterization and antibacterial activity," *Journal of Alloys and Compounds*, vol. 710, pp. 302–311, 2017.

[5] M. Silva-Ichante, Y. Reyes-Vidal, F. J. Bácame-Valenzuela et al., "Electrodeposition of antibacterial Zn-Cu/silver nanoparticle (AgNP) composite coatings from an alkaline solution containing glycine and AgNPs," *Journal of Electroanalytical Chemistry*, vol. 823, pp. 328–334, 2018.

[6] A. Panaćek, R. Prucek, J. Hrbać et al., "Polyacrylate-assisted size control of silver nanoparticles and their catalytic activity," *Chemistry of Materials*, vol. 26, no. 3, pp. 1332–1339, 2014.

[7] M. Shabaninezhad and G. Ramakrishna, "Theoretical investigation of plasmonic properties of quantum-sized silver nanoparticles," *Plasmonics*, vol. 15, no. 3, pp. 783–795, 2020.

[8] Y. Lin, Y.-J. Zhang, W.-M. Yang et al., "Size and dimension dependent surface-enhanced Raman scattering properties of well-defined Ag nanocubes," *Applied Materials Today*, vol. 14, pp. 224–232, 2019.

[9] C. Kinnear, T. L. Moore, L. Rodriguez-Lorenzo, B. Rothen-Rutishauser, and A. Petri-Fink, "Form follows function: nanoparticle shape and its implications for nanomedicine," *Chemical Reviews*, vol. 117, no. 17, pp. 11476–11521, 2017.

[10] A. Haider and I.-K. Kang, "Preparation of silver nanoparticles and their industrial and biomedical applications: a comprehensive review," *Advances in Materials Science and Engineering*, vol. 2015, Article ID 165257, 16 pages, 2015.

[11] S. Mozaffari, W. Li, C. Thompson et al., "Colloidal nanoparticle size control: experimental and kinetic modeling investigation of the ligand-metal binding role in controlling the nucleation and growth kinetics," *Nanoscale*, vol. 9, no. 36, pp. 13772–13785, 2017.

[12] L. Xing, Y. Xiahou, P. Zhang, W. Du, and H. Xia, "Size control synthesis of monodisperse, quasi-spherical silver nanoparticles to realize surface-enhanced Raman scattering uniformity and reproducibility," *ACS Applied Materials & Interfaces*, vol. 11, no. 19, pp. 17637–17646, 2019.

[13] L. Marciniak, M. Nowak, A. Trojanowska, B. Tylkowski, and R. Jastrzab, "The effect of pH on the size of silver nanoparticles obtained in the reduction reaction with citric and malic acids," *Materials*, vol. 13, no. 23, pp. 5444–5455, 2020.

[14] S. Das, K. Bandyopadhyay, and M. M. Ghosh, "Effect of stabilizer concentration on the size of silver nanoparticles synthesized through chemical route," *Inorganic Chemistry Communications*, vol. 123, Article ID 108319, 2021.

[15] J. Polte, "Fundamental growth principles of colloidal metal nanoparticles—a new perspective," *CrystEngComm*, vol. 17, no. 36, pp. 6809–6830, 2015.

[16] L. A. Jasem, A. A. Hameed, M. A. Al-Heety, A. R. Mahmood, A. Karadağ, and H. Akbaş, "The mixture of silver nanosquare and silver nanohexagon: green synthesis, characterization and kinetic evolution," *Materials Reseach Express*, vol. 6, no. 8, Article ID 0850f9, 2019.

[17] N. T. K. Thanh, N. Maclean, and S. Mahiddine, "Mechanisms of nucleation and growth of nanoparticles in solution," *Chemical Reviews*, vol. 114, no. 15, pp. 7610–7630, 2014.

[18] K. V. Kinhal, N. Bhatt, and P. Subramaniam, "Transport and kinetic effects on the morphology of silver nanoparticles in a millifluidic system," *Industrial & Engineering Chemistry Research*, vol. 58, no. 15, pp. 5820–5829, 2019.

[19] P. Singh, R. W. Carpenter, and D. A. Buttry, "Electrochemical cycling of polycrystalline silver nanoparticles produces single-crystal silver nanocrystals," *Langmuir*, vol. 33, no. 47, pp. 13490–13495, 2017.

[20] C. M. Fox, T. Yu, and C. B. Breslin, "Electrochemical formation of silver nanoparticles and their catalytic activity immobilised in a hydrogel matrix," *Colloid and Polymer Science*, vol. 298, no. 6, pp. 549–558, 2020.

[21] D. T. Thuc, T. Q. Huy, L. H. Hoang et al., "Green synthesis of colloidal silver nanoparticles through electrochemical method and their antibacterial activity," *Materials Letters*, vol. 181, pp. 173–177, 2016.

[22] A. Cojocaru, O. Brincoveanu, A. Pantazi et al., "Electrochemical preparation of Ag nanoparticles involving choline chloride—glycerol deep eutectic solvents," *Bulgarian Chemical Communications*, vol. 49, pp. 194–204, 2017.

[23] O. I. Kuntyi, A. R. Kytsya, I. P. Mertsalo et al., "Electrochemical synthesis of silver nanoparticles by reversible current in solutions of sodium polyacrylate," *Colloid and Polymer Science*, vol. 297, no. 5, pp. 689–695, 2019.

[24] O. Kuntyi, A. Mazur, A. Kytsya et al., "Electrochemical synthesis of silver nanoparticles in solutions of rhamnolipid," *Micro & Nano Letters*, vol. 15, no. 12, pp. 802–807, 2020.

[25] V. Sáez and T. Mason, "Sonoelectrochemical synthesis of nanoparticles," *Molecules*, vol. 14, no. 10, pp. 4284–4299, 2009.

[26] G. Yang and J.-J. Zhu, "Sonoelectrochemical synthesis and characterization of nanomaterials," in *Handbook of Ultrasonics and Sonochemistry,*, M. Ashokkumar, Ed., Springer, Singapore, 2016.

[27] M. Murtaza, N. Hussain, H. Ya, and H. Wu, "High purity copper nanoparticles via sonoelectrochemical approach," *Materials Research Express*, vol. 6, no. 11, Article ID 115058, 2019.

[28] K. Zhang, S. Yao, G. Li, and Y. Hu, "One-step sonoelectrochemical fabrication of gold nanoparticle/carbon nanosheet hybrids for efficient surface-enhanced Raman scattering," *Nanoscale*, vol. 7, no. 6, pp. 2659–2666, 2015.

[29] C. He, L. Liu, Z. Fang, J. Li, J. Guo, and J. Wei, "Formation and characterization of silver nanoparticles in aqueous solution via ultrasonic irradiation," *Ultrasonics Sonochemistry*, vol. 21, no. 2, pp. 542–548, 2014.

[30] O. Kuntyi, M. Shepida, M. Sozanskyi et al., "Sonoelectrochemical synthesis of silver nanoparticles in sodium polyacrylate solution," *Biointerface Research in Applied Chemistry*, vol. 11, no. 4, pp. 12202–12214, 2021.

[31] J. Zhu, S. Liu, O. Palchik, Y. Koltypin, and A. Gedanken, "Shape-controlled synthesis of silver nanoparticles by pulse sonoelectrochemical methods," *Langmuir*, vol. 16, no. 16, pp. 6396–6399, 2000.

[32] J.-J. Zhu, Q.-F. Qiu, H. Wang, J.-R. Zhang, J.-M. Zhu, and Z.-Q. Chen, "Synthesis of silver nanowires by a sonoelectrochemical method," *Inorganic Chemistry Communications*, vol. 5, no. 4, pp. 242–244, 2002.

[33] Y. Socol, O. Abramson, A. Gedanken, Y. Meshorer, L. Berenstein, and A. Zaban, "Suspensive electrode formation in pulsed sonoelectrochemical synthesis of silver nanoparticles," *Langmuir*, vol. 18, no. 12, pp. 4736–4740, 2002.

[34] L.-P. Jiang, A.-N. Wang, Y. Zhao, J.-R. Zhang, and J.-J. Zhu, "A novel route for the preparation of monodisperse silver nanoparticles via a pulsed sonoelectrochemical technique," *Inorganic Chemistry Communications*, vol. 7, no. 4, pp. 506–509, 2004.

[35] S. Tang, X. Meng, H. Lu, and S. Zhu, "PVP-assisted sonoelectrochemical growth of silver nanostructures with various shapes," *Materials Chemistry and Physics*, vol. 116, no. 2-3, pp. 464–468, 2009.

[36] L. V. Vu, N. N. Long, S. C. Doanh, and B. Q. Trung, "Preparation of silver nanoparticles by pulse sonoelectrochemical method and studying their characteristics," *Journal of Physics: Conference Series*, vol. 187, Article ID 012077, 2009.

[37] S. J. Varjani and V. N. Upasani, "Critical review on biosurfactant analysis, purification and characterization using rhamnolipid as a model biosurfactant," *Bioresource Technology*, vol. 232, pp. 389–397, 2017.

[38] R. Yamasaki, A. Kawano, Y. Yoshioka, and W. Ariyoshi, "Rhamnolipids and surfactin inhibit the growth or formation of oral bacterial biofilm," *BMC Microbiology*, vol. 20, no. 1, Article ID 358, 2020.

[39] N. Hamzah, N. Kasmuri, W. Tao, N. Singhal, L. Padhye, and S. Swift, "Effect of rhamnolipid on the physicochemical properties and interaction of bacteria and fungi," *Brazilian Journal of Microbiology*, vol. 51, no. 3, pp. 1317–1326, 2020.

[40] F. J. Ochoa-Loza, J. F. Artiola, and R. M. Maier, "Stability constants for the complexation of various metals with a rhamnolipid biosurfactant," *Journal of Environmental Quality*, vol. 30, no. 2, pp. 479–485, 2001.

[41] D. E. Hogan, J. E. Curry, J. E. Pemberton, and R. M. Maier, "Rhamnolipid biosurfactant complexation of rare earth elements," *Journal of Hazardous Materials*, vol. 340, pp. 171–178, 2017.

[42] O. Hari and S. K. Upadhyay, "Rhamnolipid-metal ions (Cr VI and Pb II) complexes: spectrophotometric, conductometric, and surface tension measurement studies," *Journal of Surfactants and Detergents*, vol. 24, no. 2, pp. 281–288, 2020.

[43] S. A. Kornii, V. I. Pokhmurs'kyi, V. I. Kopylets, I. M. Zin, and N. R. Chervins'ka, "Quantum-chemical analysis of the electronic structures of inhibiting complexes of rhamnolipid with metals," *Materials Science*, vol. 52, no. 5, pp. 609–619, 2017.

[44] Y. Xie, R. Ye, and H. Liu, "Synthesis of silver nanoparticles in reverse micelles stabilized by natural biosurfactant," *Colloids and Surfaces A: Physicochemical and Engineering Aspects*, vol. 279, no. 1–3, pp. 175–178, 2006.

[45] C. G. Kumar, S. K. Mamidyala, B. Das, B. Sridhar, G. S. Devi, and M. S. Karuna, "Synthesis of biosurfactant-based silver nanoparticles with purified rhamnolipids isolated from pseudomonas aeruginosa BS-161R," *Journal of Microbiology and Biotechnology*, vol. 20, no. 7, pp. 1061–1068, 2010.

[46] L. Bazylyak, A. Kytsya, O. Karpenko et al., "Synthesis of silver nanoparticles using the rhamnolipid biocomplex of microbial origin," *Visnyk of the Lviv University. Series Chemistry*, vol. 61, no. 2, pp. 404–413, 2020.

[47] S. Dwivedi, Q. Saquib, A. A. Al-Khedhairy, J. Ahmad, M. A. Siddiqui, and J. Musarrat, "Rhamnolipids functionalized AgNPs-induced oxidative stress and modulation of toxicity pathway genes in cultured MCF-7 cells," *Colloids and Surfaces B: Biointerfaces*, vol. 132, pp. 290–298, 2015.

[48] C. T. Rueden, J. Schindelin, M. C. Hiner et al., "ImageJ2: ImageJ for the next generation of scientific image data," *BMC Bioinformatics*, vol. 18, no. 1, Article ID 529, 2017.

[49] F. You, W. Tang, and L.-Y. L. Yung, "Real-time monitoring of the trojan-horse effect of silver nanoparticles by using a genetically encoded fluorescent cell sensor," *Nanoscale*, vol. 10, no. 16, pp. 7726–7735, 2018.

[50] S. J. Nurani, C. K. Saha, M. A. R. Khan, and S. M. H. Sunny, "Silver nanoparticles synthesis, properties, applications and future perspectives: a short review," *IOSR Journal of Electrical and Electronics Engineering*, vol. 10, no. 6, pp. 117–126, 2015.

[51] Y. Matsumura, K. Yoshikata, S.-i. Kunisaki, and T. Tsuchido, "Mode of bactericidal action of silver zeolite and its comparison with that of silver nitrate," *Applied and Environmental Microbiology*, vol. 69, no. 7, pp. 4278–4281, 2003.

[52] J. R. Morones, J. L. Elechiguerra, A. Camacho et al., "The bactericidal effect of silver nanoparticles," *Nanotechnology*, vol. 16, no. 10, pp. 2346–2353, 2005.